Published in final edited form as:
Nat Microbiol. 2019 December ; 4(12): 2164–2174. doi:10.1038/s41564-019-0568-5.

Escherichia coli limits *Salmonella* Typhimurium infections after diet-shifts and fat-mediated microbiota perturbation in mice

Sandra Y. Wotzka[1], **Markus Kreuzer**[1], **Lisa Maier**[2], **Markus Arnoldini**[1], **Bidong Nguyen**[1], **Alexander O. Brachmann**[1], **Dorothée L. Berthold**[1], **Mirjam Zünd**[1], **Annika Hausmann**[1], **Erik Bakkeren**[1], **Daniel Hoces**[1], **Ersin Gül**[1], **Markus Beutler**[3], **Tamas Dolowschiak**[1], **Michael Zimmermann**[5], **Tobias Fuhrer**[5], **Kathrin Moor**[1], **Uwe Sauer**[5], **Athanasios Typas**[2], **Jörn Piel**[1], **Médéric Diard**[1], **Andrew J. Macpherson**[6], **Bärbel Stecher**[3,4], **Shinichi Sunagawa**[1], **Emma Slack**[1], **Wolf-Dietrich Hardt**[1,*]

[1]Institute of Microbiology, D-BIOL, ETH Zürich, CH-8093 Zürich, Switzerland [2]European Molecular Biology Laboratory, Heidelberg, Meyerhofstraße 1, Heidelberg, 69117, Germany [3]Max von Pettenkofer Institute, Faculty of Medicine, LMU Munich. Pettenkoferstrasse 9a, D-80336 Munich, Germany [4]German Center for Infection Research (DZIF), Partner site Munich [5]Institute of Molecular Systems Biology, D-BIOL, ETH Zürich, CH-8093 Zürich, Switzerland [6]Maurice Müller Laboratories, University Clinic for Visceral Surgery and Medicine, University of Bern, Bern, Switzerland

Summary

The microbiota confers colonization resistance, which blocks *Salmonella* gut colonization [1]. As diet affects microbiota composition, we studied whether food-composition shifts enhance susceptibility to infection. Shifting mice to diets with reduced fiber or elevated fat contents for 24h boosted *S.* Typhimurium or *E. coli* gut colonization and plasmid transfer. Here, we studied the effect of dietary fat. Colonization resistance was restored within 48h of return to maintenance diet.

Correspondence to: Wolf-Dietrich Hardt, Institute of Microbiology, Vladimir-Prelog-Weg 4, CH-8093 Zürich, Switzerland, Tel: + +41-44-632-5143; hardt@micro.biol.ethz.ch.

Ethical Statement
All animal experiments were reviewed and approved by the Kantonales Veterinäramt, Zürich (license 222/2013 + 193/2016) and are subject to the Swiss animal protection law (TschG).

Data Availability
16S rRNA raw reads have been deposited at the European Nucleotide Archive (ENA), with accession number PRJEB33890. All other data needed to evaluate the conclusions in this Article are presented in the paper or the Supplementary Information. Any additional data can be requested from the corresponding author.

Author contributions
S.Y.W. (figure 1-3, S2-S5, S8-S7, S10-S11, S16, S18, S22-S23), B.N. (figure S24), L.M. and A.T. (figure 2e, S12), A.O.B. and J.P. (figure 2a), M.A. (figure 3a-b, S13-S15), D.L.B. (figure S19, S21b, table S4-S5), M.Zü. and S.S. (figure S7, S26), A.H. (figure S21a), E.B. and M.D. (figure 1e, S6), K.M. (figure 1b-d), M.K. (figure 4, S4, S17, S18G, S25), D.H. and E.S. (figure 2d, S23), M.B. and B.S. (figure S7b), T.D. (figure S19), M.Zi., T.F. and U.S. (figure S9, S18a-b,f), E.G. (S20), A.J.M and B.S. (Oligo mice) performed the experiments and analyzed the data. S.Y.W., M.K. contributed equally. S.Y.W., M.K., B.N., L.M., D.H., E.S. and W.-D. H. designed the experiments, S.Y.W., M.K. and W.-D.H. wrote the manuscript.

Competing Interests statement
The authors declare no competing financial interests.

Europe PMC Funders Author Manuscripts

Salmonella gut colonization was also boosted by two oral doses of oleic acid, or bile salts. These pathogen blooms required *Salmonella*'s AcrAB/TolC-dependent bile-resistance. Our data indicate that fat-elicited bile is promoting *Salmonella* gut colonization. Both, *E. coli* and *Salmonella* show much higher bile resistance than the microbiota. Correspondingly, competitive *E. coli* can be protective in the fat-challenged gut. Diet shifts and fat-elicited bile promote *S.* Typhimurium gut infections in mice lacking *E. coli* in their microbiota. This mouse model may be useful for studying pathogen-microbiota-host interactions, the protective effect of *E. coli,* for analyzing the spread of resistance plasmids and for assessing the impact of food components on the infection process.

We hypothesized that diet-composition shifts might affect colonization resistance, as 24-48h on diets with elevated fat- or reduced fiber-content suffice to alter microbiota compositions and fiber-deprivation accelerates murine *Citrobacter rodentium* infections [2,3]. We initially analyzed a typical high-fat Western-type diet without fiber (WD; figure 1a). C57BL/6 mice harboring an unperturbed, complex, *E. coli*-free microbiota (CON^E; table S1) were reared on a standard plant-based maintenance diet (MD). Mice remaining on MD limited gut-luminal *S.*Tm SL1344 growth (figure 1b). In spite of possible batch-to-batch variations, this colonization resistance has been consistent over many years [4]. Another group was shifted to WD 24h before per-oral inoculation with *S.*Tm (figure 1a-d). Strikingly, this group featured 10^2-10^5 fold higher stool pathogen loads than the MD controls (figure 1b). Stool pathogen loads rose almost as quickly, as in antibiotic pre-treated animals [4]. Also, WD-shifted mice showed elevated gut luminal pathogen loads, exacerbated systemic infection and increased enteropathy by 96h p.i. (figure 1c,d). Shifts to WD also promoted *S.*Tm gut colonization in C57BL/6 mice carrying a defined *E. coli*-free consortium (Oligo [5]), C57BL/6 mice carrying another complex microbiota (CON^R, includes *E. coli*) and 129SvEv mice (CON^X microbiota, no *E. coli*; figure S2a-d, table S1). Furthermore, WD-shifts boosted gut colonization by a second *wt S.* Typhimurium strain (ATCC14028; see below in figure S6), the mouse commensal *E. coli* 8178 [6] (figure S2e) and by *S.*Tm^{avir}, an avirulent *S.*Tm mutant (figure S3, table S2), which grows luminally without eliciting enteropathy. *S.*Tm blooms were also observed after shifts to a fiber-containing high-fat diet, but not the low-fat control (figure S4). Thus, fat might be involved. As fiber-free low-fat diet also enhanced *S.*Tm colonization (figure S4), we conclude that gut luminal growth of *S.*Tm and other *Enterobacteriaceae* is promoted not only by fiber-deprivation, as reported previously [3], but also by fat and possibly other unidentified food constituents.

We decided to focus on the role of fat, as associated microbiota changes and disease phenotypes hinted at this nutrient as one possible trigger of enterobacteriaceal blooms [2,7–9]. First, we supplemented MD with additional lard. Shifts to this diet promoted *S.*Tm gut colonization (figure S2f). Then, we gavaged mice on MD with oleic acid. This unsaturated fatty acid does not elicit inflammatory responses [10] and is a main digestive breakdown product of lard (≈45%). In mice on MD, oleic acid doses of as little as ≈0.4ml/kg body weight raised pathogen stool loads by 10-fold ($p<0.05$; 2x10µl; figure S5). This corresponds to doses of ≈60g of animal fat for a 70kg person. Human high-fat diets can include >150g fat per day. Doses of >2x10µl oleic acid boosted gut luminal *S.*Tm colonization by 10^4-fold and significantly aggravated *S.*Tm-inflicted disease (figure 1a-d, figure S2a,b, figure S5).

Thus, short exposures to fat or oleic acid can promote *S.*Tm blooms, at least in *E. coli* free mice.

Dysbiosis-mediated enterobacteriaceal blooms can fuel the spread of resistance plasmids [11]. To test if WD-shift or oleic acid-promoted blooms have a similar effect, we studied transfer rates of plasmid PII from *S.*Tm SL1344 (i.e. PII^{CmR} carrying a chloramphenicol resistance). PII belongs to an IncI1-family of antibiotic resistance- and colicin plasmids commonly found in *Enterobacteriaceae* [6]. Mice were sequentially infected with the recipient strain (*S.*Tm $ATCC14028^{KmR}$) and 15 minutes later with the donor (*S.*Tm SL1344, PII^{CmR}). Indeed, WD-shift and oleic acid boosted plasmid transfer by 10^2-10^6-fold compared to controls (figure 1e, figure S6). It remains unclear, if this is solely attributable to increased donor/recipient densities.

The microbiota composition changed 12-24h after WD-shift or oleic acid gavage (figure S7). This provided a hint that microbiota disturbance might explain the elevated susceptibility to *S.*Tm. The alleviation of colonization resistance was transient. After return to MD, the mice regained full colonization resistance within 24-44h (figure 1g, figure S8). Therefore, our subsequent mechanistic analysis focused on the time-window of 0-24h after the dietary perturbation.

Next, we tested, if bile salts might be involved. Fat digestion necessitates bile salt release into the gut lumen [12,13]. While most bile is resorbed before passage into the large intestine, fecal concentrations can reach ≈0.3% (w/v) after fat consumption [14]. Indeed, bile salts were elevated in the cecal contents after the WD-shift or oleic acid gavage (figure S9). Cholate, a primary bile salt, reached concentrations of up to 0.1% (figure 2a). These data hinted at bile salt-mediated alleviation of colonization resistance, as bile salts are well-known inhibitors for numerous bacterial species [15,16], but not *Salmonella* or *E. coli* spp. [17]. This has been utilized in stool diagnostics, which traditionally employs bile-supplements to culture *Salmonella* or *E. coli* spp. while suppressing unwanted microbes [18]. To establish the role of bile salts in alleviating colonization resistance, we administered cholate by oral gavage at 1 hour before and 4 hours after infection. Two doses of cholate (100µl, 8%) promoted *S.*Tm gut colonization almost as efficiently as streptomycin (streptomycin *S.*Tm enterocolitis model [4]; figure 2b,c), while gut transit times remained unaltered (figure S10). Taurocholate, another primary bile salt, had a similar effect (figure S11). Thus, bile salts alone can elicit *S.*Tm blooms independent of dietary fat.

The microbiota were more sensitive to bile salts than wt *S.*Tm or *E. coli*. This was established by life/dead-dye exclusion from cholate-exposed gut luminal bacteria (figure 2d) and by cholate-inhibition of the anaerobic growth of 16 representative strains isolated from human and 9 strains from murine stools (from Oligo-microbiota; table S3). Most microbiota strains were inhibited by ≥0.125% cholate (figure 2e). In contrast, wt *S.*Tm and the human commensal *E. coli* ED1a were ≈10-fold more resistant than the microbiota or mutants lacking the AcrAB/TolC efflux pump, a known determinant of enterobacteriaceal bile resistance [19,20] (figure 2d,e; table S2; table S4; table S5). Equivalent observations were made with taurocholate (figure S12). Thus, bile salts are sufficient to re-capitulate the loss of colonization resistance associated with WD-shift or oleic acid treatment.

To assess quantitatively if bile-inflicted differences in growth rates are sufficient to explain why fat promotes *S.*Tm blooms, we formulated a mathematical model and used it to generate explicit predictions. Specifically, we modeled the outcome of competition (for colonizing the cecum lumen) between *S.*Tm and a generic microbiota after 24h, using the bile-salt dependent growth parameters derived from figure 2e (see Supplementary Material on the model for details; table S6, figure S13, figure S14, figure S15). This recapitulated the behavior of our system. Wt *S.*Tm outcompeted the microbiota at bile salt concentrations realistic in the fat-exposed cecum, whereas the microbiota stayed dominant at bile salt concentrations below 0.15% (figure 3a). In contrast, an *acrAB* mutant could not efficiently out-compete the microbiota even at high bile salt concentrations (*S.*Tm^{acrAB}; figure 3b). Thus, bile salt-mediated growth inhibition is sufficient to explain why WD, dietary fat and oleic acid promote gut infection.

This was verified by competitive infection experiments of wt *S.*Tm vs. *acr* mutants that feature a similar bile salt sensitivity as most Bacteroidetes or Firmicutes strains (figure 2e). When WD-shift, oleic acid or cholate were applied (but not in the MD controls), wt *S.*Tm out-competed the *acr* mutants (figure 3c,d; figure S16; figure S17). In keeping, *S.*Tm^{acrAB} yielded lower gut luminal densities than wt *S.*Tm after WD-shifts. To further assess the colonization defect of *S.*Tm^{acrAB}, we infected mice after WD-shifts with one *S.*Tm strain at a time (figure 3e). These data establish bile-resistance as a key factor promoting *Enterobacteriacea* blooms in the fat-exposed gut.

Control experiments assessed if pathogen growth on fatty acids may fuel *S.*Tm blooms in the fat-exposed gut. However, cecal long-chain fatty acid (LCFA) concentrations remained unchanged after WD-shift or oleic acid gavage (figure S18a,b). Moreover, *S.*Tm^{fadL} which is deficient in LCFA uptake (Δ*fadL*) showed only a minor gut luminal growth attenuation (≤2-fold; figure S18e). This defect was much smaller than the 10^3 to 10^4-fold growth difference of *S.*Tm^{WT} between WD- or oleic acid-exposed mice and animals on MD (figure S18e). Similarly, we could exclude cross-feeding on products from other microbiota, like short-chain fatty acids (SCFA, acetate, propionate, butyrate; figure S18f-i). In conclusion, fatty acid utilization by *S.*Tm is not necessary for pathogen growth in the fat-exposed gut.

A second set of controls assessed if fat exposure might elicit gut inflammation and thereby enhance pathogen growth [8,21–26]. However, within 24h, neither WD-shift, nor gavage with oleic acid or cholate affected cardinal mucosal inflammation marker expression, T_{reg}-or phagocyte numbers implicated in disease-fueled *Salmonella* growth [26] (figure S19, figure S20, figure S21). Thus, sub-acute inflammatory responses are dispensable for the alleviation of colonization resistance. While IL-22 is dispensable in our model (figure S22), it may contribute in other situations, as some animals featured elevated *il-22* and *reg-IIIβ*, an antimicrobial peptide favoring enterobacteriaceal blooms [27–29](figure S19).

Further controls verified that expression of SPI-1, an inflammation-triggering virulence factor, was unaffected upon WD-shift or oleic acid gavage (figure S23). Finally, competitive infections verified that nitrate respiration (as needed for *S.*Tm growth in the inflamed gut [30]) was dispensable for accelerating growth in mice subjected to WD-shift or oleic acid (C.I. ≈

1; figure S24). Thus, mucosal inflammation is not required for fat-mediated promotion of *S.*Tm gut colonization (figure S1, step 1b).

Finally, we assessed if *E. coli* may limit *S.*Tm infections after diet-shifts. Wt *E. coli* strains are common members of animal microbiota, encode AcrAB/TolC, are bile resistant, and bloom after WD-shift (figure 2e, figure S2e, figure S12) [31–33]. Moreover, some, but not all, *E. coli* strains are capable of outcompeting *Salmonella* spp. in the gut of mice and chickens [6,34]. Correspondingly, *S.*Tm blooms were ≈10-1000-fold smaller when the microbiota includes a *Salmonella*-competitive *E. coli* (compare figure 1b vs figure S2c; table S1). Therefore, competitive *E. coli* might limit fat-promoted pathogen blooms. CON^E mice were gavaged with oleic acid or shifted to WD as in figure 1a and co-infected with wt *S.*Tm and a mixture of three *E. coli* strains ($5x10^7$ cfu, by gavage; table S2; figure 4a,b) capable of growth in 2% cholate. *E. coli* 8178 and CFT073 can out-compete *S.*Tm in antibiotic treated mice [6] and *E. coli* Z1324 is a recent isolate from a healthy human volunteer [33]. Indeed, the *E. coli* mix colonized the murine gut, suppressed oleic acid- and WD-promoted *S.*Tm blooms by 10^2-10^5-fold and prevented enteropathy (figure 4a-c).

Within the *E. coli* mix, *E. coli* 8178 achieved the highest gut luminal densities. Indeed, *E. coli* 8178 alone could limit gut luminal *S.*Tm blooms after a WD-shift for 72-96h. It did not matter, whether *E. coli* 8178 was applied in parallel, or 48 hours before the *S.*Tm infection (figure 4d, figure S25). However, *E. coli* 8178 alone was less efficient than the *E. coli* mix. We conclude that competitive *E. coli* can preserve colonization resistance after fat-mediated disturbance.

This work identifies fat as one factor promoting *Salmonella* diarrhea in mice. Fat can achieve this by eliciting bile salts which are well tolerated by *S.*Tm or *E. coli* but not by most Bacteroidetes or Firmicutes strains. Experimental data and modeling indicate that bile salts, which are released during fat digestion, can ablate colonization resistance, i.e. when competitive *E. coli* strains are missing. The high prevalence of *E. coli* spp. may explain, why Western-type diets are not associated with human *Salmonella* diarrhea (supplementary discussion). *E. coli* presence and their exact genetic make-up may determine whether colonization resistance is maintained during microbiota disturbance, or not. Future studies should assess the relevant competitive mechanisms (e.g. colicins, type 6 secretion systems, oxygen- or iron-depletion [5,34–38]). Such knowledge might help to identify individuals at risk, and to prevent infections by supplementing potent competitive *E. coli* strains. However, colonization resistance can also be achieved without *E. coli*, as indicated by our experiments in unperturbed CON^E mice. Nevertheless, when WD-shifts or oleic acid exposure disturb the microbiota, *E. coli* can promote resilience, invigorating colonization resistance after perturbations.

*S.*Tm growth in the fat-digesting gut relies on AcrAB/TolC efflux pumps [19,20,39,40]. Most likely, this also holds true for other *Enterobacteriaceae* like *Citrobacter*, *Escherichia*, *Salmonella*, *Enterobacter*, *Yersinia, Klebsiella, or Shigella* spp.. Of note, bile resistance is further modulated by additional factors [41], bile can promote pathogen germination [42] and distant *acrAB*-like genes are also present in other bacteria (figure S26). Deciphering their contribution to fat/bile-elicited pathogen blooms will be an interesting topic for future work.

Colonization resistance is also compromised by mechanisms other than bile-salt-mediated microbiota perturbation. In cases of fat-exposure, pathogen growth on long-chain fatty acids, and elicitation of IL-22-elicited antimicrobial peptides might contribute in some cases, in particular in the long term. However, in most mice, pathogen growth in the fat-exposed gut begins in the absence of inflammation (figure S1, step 1b). Fiber-deprivation can also promote *C. rodentium* [3] and *S.*Tm blooms (figure S4). Most likely, additional factors can also alleviate colonization resistance and remain to be identified.

Finally, our findings impinge on the spread of antibiotic resistance plasmids, which is currently of major concern (WHO, 2017) [43]. As conjugation is contact-dependent and therefore promoted by high donor and recipient densities [11], enterobacteriaceal blooms elicited by inflammation or antibiotics are known to fuel this process [6]. Our findings suggest that under certain circumstances, diet-shifts may fuel such bloom-driven plasmid transfer.

We conclude that dietary-shifts can serve to study the microbiota-pathogen-host interaction in mice. This may be useful for research on acute infections, protective *E. coli* strains and resistance plasmid spread.

Methods

Bacterial strains

S. enterica serovar Typhimurium strains used in this study are generally derivatives of the wt strain SL1344 (SB300) [44]. The recipient in PII conjugation experiments was a derivative of *S.*Tm ATCC14028. Deletions in the acetate and propionate metabolism (Δ*aceA* + Δ*prpBCDE*), a key determinant of fatty acid uptake (Δ*fadL*) and components of the multidrug efflux pump AcrAB-TolC and AcrAD-TolC were constructed using the lambda/red homologous recombination technique [45]. For selection, the *cat* cassette from pKD3 or the *aphT* cassette from pKD4 were chosen to replace the open reading frames of interest by double homologous recombination. Mutated alleles were subsequently transduced into a fresh strain background by P22 phage transduction. Wt isogenic tagged strains (WITS) were kindly provided by A.J. Grant [46]. Tags were transduced into the mutant strains deficient in acetate and propionate metabolism (Δ*aceA* + Δ*prpBCDE*), the long-chain fatty acid import protein (Δ*fadL*), the multidrug efflux pump AcrAB-TolC and AcrAD-TolC, using P22 phage transduction and subsequent selection on kanamycin or chloramphenicol. Tagged strains were used in competitive infection experiments to test up to six mutant strains against the wt in a given mouse. If indicated, the resistance cassette was removed using pCP20 encoded flippase to generate strains harboring an in frame deletion. The replication-incompetent ColE1-like plasmid pAM34 was used to determine the growth rate of *S.*Tm and have been described previously [47–49]. The plasmid pM972 (p*sicA-gfp*) was used to quantify SPI-1 expression in *S.*Tm and have been described previously [50]. The *sicA* promoter (p*sicA*) thereby controls the expression of the chromosomal *sicAsipBCDA* operon, which encodes key parts of the SPI-1 Type 3 secretion system (T3SS-1). In addition, the mouse commensal *Escherichia coli* 8178 [6] was used in infection experiments. All constructs were verified by PCR and all strains and their corresponding genotype are listed in table S2.

Ex vivo growth conditions

For infection experiments, bacteria were grown for 12h at 37°C shaking (160 rpm) in LB broth and the appropriate antibiotics, sub-cultured for 4h in LB broth containing 0.3 M NaCl without antibiotics using the same growth conditions und re-suspended in PBS as described previously [4].

For the minimal inhibitory concentration assays, bacteria were grown overnight at 37°C shaking (160 rpm) in LB broth containing the appropriate antibiotics. Cultures were adjusted to an OD_{600} of 1 and further diluted 1:2000 in LB broth to reach 10^4 CFU per tested condition.

Animals

Male and female 8-to-12-week-old mice were used. The mouse lines used, their microbiota and the presence of *E. coli* is summarized in table S1. All mice were bred under specific (opportunistic and) pathogen-free (SPF, SOPF) conditions in individually ventilated cages in the Rodent Center HCI (RCHCI) or the EPIC mouse facility of ETH Zurich, Switzerland. Briefly, the CON^R microbiota harbors a commensal *E. coli* streptomycin-sensitive strain. CON^E mice were re-derived by artificial insemination into a SOPF foster colony and bred in full barrier conditions in individually ventilated cages in the ETH Phenomics centre (EPIC) (Zurich, Switzerland). 129 Sv/Ev mice (CON^X) were bred in full barrier SOPF conditions in individually ventilated cages in the EPIC facility of ETH Zurich, Switzerland (no *E. coli* strains detectable). Oligo (12 strain microbiota; C57BL/6) mice are ex-germ-free mice, which were colonized with a defined consortium of 12 bacterial strains isolated from the murine gut (no *E. coli* strains). These mice are also designated as stable Defined Moderately Diverse Microbiota mouse (sDMDMm2) were generated in a collaboration between Prof. Stecher, Prof. McCoy and Prof. Macpherson (University of Bern) [5,51]. The Oligo mice were bred in open top cages within flexible film isolators under strict hygienic isolation in a separate room of the EPIC (Zurich, Switzerland; no *E. coli* strains).

All mice were maintained on the mouse maintenance diet (symbol: ●, MD, Kliba Nafag, 3537; autoclaved; per weight: 4.5% fat, 18.5% protein, ≈50% carbohydrates, 4.5% fiber). As indicated, mice were shifted to a Western-type diet without fiber (symbol: △, WD, BioServ, S3282; 60% kcal fat; irradiated; per weight: 36% fat, 20.5% protein, 35.7% carbohydrates, 0% fiber), control diet without fiber (symbol: ▲, BioServ, S4031; 16% kcal fat; irradiated; per weight: 7.2% fat, 20.5% protein, 61.6% carbohydrates, 0% fiber), High-fat diet with fiber (symbol: □, ENVIGO, TD.06414; 60% kcal fat; irradiated; per weight: 34.3% fat, 23.5% protein, 27.3% carbohydrates, 6.6% fiber) or control diet with fiber (symbol: ■, ENVIGO, TD.08806; 10.5% kcal fat; irradiated; per weight: 4.2% fat, 18.6% protein, 62.6% carbohydrates, 3.7% fiber) which were fed ad libitum.

Infections and Competitive Infection Experiments

Infections with individual strains, or coinfection experiments with the indicated strain mixtures, were carried out in 8- to 12-weeks old mice (age- and sex-matched). Mice were kept on MD or switched to WD 24h before oral infection with $5x10^7$ CFU *S.*Tm. Additional experimental groups were treated with PBS or 200 µl, 100 µl, 50 µl or 10 µl of oleic acid, as

indicated (100 µl was used as standard protocol; Sigma-Aldrich) or 4%, 6% or 8% cholate (as indicated; cholic acid sodium salt was suspended in PBS and sterile-filtered; 8% were used as standard protocol; EMD Millipore Corp.; the dose of 100 µl 8% corresponds to 320 mg/kg body weight) or 12% taurocholate (taurocholic acid sodium salt was suspended in PBS and sterile-filtered; Sigma-Aldrich) 1 hour before and 4 hours after oral infection with $5x10^7$ CFU *S.*Tm. Pretreatment controls with 25 mg streptomycin or ampicillin were performed where indicated, as described previously [4].

Mouse experiments and data analysis was performed in a non-blinded fashion. To analyze pathogen loads, freshly collected fecal pellets were homogenized in PBS with steel balls in a tissue lyser (Qiagen) and plated on MacConkey agar plates (Oxoid) containing the appropriate antibiotics, as needed (50 µg/ml streptomycin, 50 µg/ml kanamycin, 15 µg/ml chloramphenicol and 20 µg/ml ampicillin). The competitive index was calculated by dividing the output ratio (CFU of the mutant/CFU of the wt) by the input ratio (CFU of the mutant/CFU of the wt) of the inoculum. For analysis of bacterial loads in the organs, mice were sacrificed by cervical dislocation at the indicated time point (untreated, day 1 post infection (p.i.), day 4 p.i.) and cecum content, mesenteric lymph nodes, spleen and liver were recovered and homogenized in PBS supplemented with 0.5% tergitol and 0.5% bovine serum albumin. Minimal detectable values were 10 CFU/g in feces and cecum content and 10 CFU/organ in the systemic organs. Each experiment was performed in at least two independent biological replicates including the indicated number of mice and the data were pooled for statistical analysis. Typically, we used at least 5-6 mice per group in order to allow analysis by non-parametric statistical tests.

Histological procedures

Pathological scores were determined in a blinded fashion, as described in an earlier study 16. In brief, samples from liver, spleen, ileum, cecum, and colon were embedded in O.C.T. (Sakura, Torrance, Calif.), snap-frozen in liquid nitrogen, and stored at -80°C. 5 µm sections were mounted on glass slides, air dried at room temperature for 2h, and stained with hematoxylin and eosin (H&E). Pathological score was determined by analyzing four markers of inflammation: (i) submucosal edema, (ii) polymorphonuclear granulocyte infiltration into the lamina propria, (iii) number of goblet cells harboring mucus-filled vacuoles, (iv) epithelial integrity. Pathological scores range from 0 to 13 arbitrary units with 0 to 3 = no or minimal inflammation, 4 to 6 = slight inflammation, 7 to 9 = moderate inflammation, and 10 to 13 = profound inflammation.

H&E pictures were taken with an Axioskop 2 plus (Carl Zeiss AG) microscope with mounted AxioCam HRc (Carl Zeiss AG) camera. AxioVision 4.8 (Carl Zeiss AG) software was used to capture images. Automatic best fit was applied for the best contrast.

Wt isogenic tagged strain analysis

Mice were infected with a uniform mixture of the mutant and the wt isogenic tagged strains (WITS) of *S.*Tm. A WITS-tag is thereby a unique 40 bp DNA sequence tag within a non-coding region of the chromosome (Grant et al., 2008). Feces and cecum content of infected mice were collected at the indicated time points (12h p.i. and 24h p.i.) and samples were

homogenized in 500 µl PBS (0.5% tergitol and 0.5% bovine serum albumin) using a tissue lyser device (Qiagen; 2 min 25 Hz). 250 µl of the homogenate was inoculated into 3 ml LB broth culture containing 50 mg/ml streptomycin to enrich for the tagged strains for 4 hours. 50 µl of a serial dilution was plated on MacCokey agar (50 mg/ml streptomycin) to quantify the density of colony forming units (CFU) within each sample. Genomic DNA from enrichment cultures was extracted using the QIAamp DNA Mini Kit (Qiagen). The relative densities of the different WITS were determined by realtime PCR quantification using tag-specific primers (Kaiser et al., 2014). The obtained ratio was multiplied by the number of CFUs recovered from selective plating to calculate the absolute loads of each tagged strain.

DNA extraction for 16S rRNA gene sequencing

Cecum content was collected from CON mice kept on the MD, switched to WD or treated with 200 µl of oleic acid and analyzed 6 hours, 12h and 24h after the switch or the treatment. Isolated cecum content samples were immediately shock frozen in liquid nitrogen and stored at -80°C. DNA was extracted using the AllPrepDNA/RNA/Protein Kit (Qiagen) with the following changes in the disruption and homogenization steps: 600 ml of RLT buffer and 3 x 4 mm metal beads were added to the tube containing the cecum content and bead-beated at 10 Hz for 2 min using the Retsch M400. To separate fibers from bacteria, samples were centrifuged at 700g for 2 min at 4°C. Supernatants containing the bacteria were transferred to a tube containing 0.9 mg of 0.1 mm of zirconia beads (OPS Diagnostics) and samples were homogenized at 25 Hz for 5 min. Before the transfer of the lysates to the QIAshreeder column (Qiagen), lysates were pre-heated to 25°C. The QIAshreeder columns were centrifuged at 13,000g for 3 min at room temperature for further homogenization. The flow-though was centrifuged for 3 min full-speed to pellet the cell debris. The supernatants were loaded on the DNA columns and DNA was extracted according the manufacturer's instructions with the modification that DNA was eluted in 100 µl EB.

Library preparation and 16S rRNA gene sequencing

The library was produced using the NEXTflex® 16S V4 Amplicon-Seq Kit 2.0 (Barcodes 1-96; Bioo Scientific). The input concentration of genomic DNA was adjusted to 30 ng/µl for each PCR reaction. The library preparation was performed following the manufacturer's instructions with the differences that the reaction volume was reduced to 25 µl per reaction and a modified primer pair was used for the first PCR reaction. Instead of the primer pair 515f-806r that is supplied with the kit, the degenerate primers 515F (5′-GTG**Y**CAGCMGCCGCGGTAA-3′) and 806rB (5'-GGACTAC**N**VGGGTWTCTAAT-3') as described in [52,53] were applied. The first PCR reaction was performed using Q5 High-Fidelity DNA Polymerase (BioConcept (NEB)) under the following cycle conditions: 1) Initial denaturation: 95°C for 4 min; 2) Denaturation: 95°C for 30 sec; 3) Annealing: 56°C for 30 sec; 4) Extension: 72°C for 90 sec; 5) final extension: 72°C for 4 min. Cycles 2-4 were repeated 8 times. After each PCR reaction, the PCR products were cleaned from oligos and nucleotides by AMPure XP magnetic beads (Beckman Coulter SA). The cleaned PCR product was eluted in 20 µl of resuspension buffer and used in a second PCR reaction with barcoded primers or for producing multiplexed samples. The quantity of the amplicons were measured using a Qubit fluorometer. The quality of the amplicons were verified using a Fragment Analyzer (Advanced analytical). The length of the amplicons after barcoding was

approximately 450bp. PCR products were adjusted to a final concentration of 60 ng DNA per 20 µl multiplexed sample. Paired end read sequencing was performed on the Illumina MiSeq platform at the Functional Genomics Center Zürich.

Analysis of microbiota composition

For CON^E mice, raw sequencing data were processed using custom scripts to execute several commands of the USEARCH software (version 9.1.13): paired reads were merged and quality-filtered using the fastq_mergepairs command with default settings. Merged reads were filtered using the fastq_filter command (-fastq_maxee 0.1) and only merged reads with perfect primer matches and a minimum length of 100 bp were selected. Sequences were de-replicated using the fastx_uniques command and clustered into operational taxonomic units (OTUs) at 97% using the cluster_otus command (-minsize 2), which also removed chimeric sequences. OTU abundances for each sample were quantified using the usearch_global command (-strand both; -id 0.97). Taxonomic annotation was performed by querying OTU sequences against the SILVA database (version 128) using the usearch_global command (-id 0.90; -maxaccepts 20; -maxrejects 500; -strand both; -top_hits_only). For Oligo mice, strain-specific qPCR measurements were transformed into relative abundances.

Further analyses were performed in RStudio (version 1.0.143 based on [R] version 3.3.3) using the libraries vegan and ggplot2. Read counts were rarefied to 20,000 reads per sample. For performing a principal component analysis, Euclidean distances after Hellinger transformation were computed between samples using the *vegdist* function.

Determination of *S.*Tm growth rates in the gut

*S.*Tm growth rates in the gut were assessed using replication-incompetent plasmid pAM34, which has been described previously [48,49]. Briefly, pAM34 is a ColE1-like vector in which the replication of the plasmid is under the control of the LacI repressor, whereby plasmid replication only occurs in the presence of isopropyl β-d-1-thiogalactopyranoside (IPTG) [47]. *S.*Tm carrying the pAM34 plasmid was therefore cultured for 12h in the presence of 1 mM IPTG in LB broth and in the absence of antibiotics. Cultures were diluted 1:20 into fresh LB broth without IPTG and sub-cultured for 3 hours at 37°C. Inocula for *in vivo* infections have been prepared as described previously [4]. Oligo mice were kept on the MD, switched to WD 24h before infection or treated with 100 µl oleic acid 1 hour before and 4 hours after the infection with $5x10^7$ CFU *S.*Tm carrying pAM34. Concurrently, the inoculum was serially diluted into fresh LB broth without IPTG and cultured overnight at 37°C to generate a standard curve relating plasmid loss to generations undergone for each experiment. pAM34 carrying bacteria within the overnight cultures and the feces were determined by selective plating on agar plates containing 100 µg/ml ampicillin and 1mM IPTG. To quantify the total population size, samples were further plated on agar plates containing 50 µg/ml streptomycin. The fraction of pAM34 carrying bacteria was calculated using the ratio of pAM34-carrying CFU to total population CFU and generations estimated by interpolation from the matched standard curve.

Real-Time qPCR for analysis of transcript levels

The cecum mid-segments were rinsed in cold sterile PBS and the washed tissue was shock frozen in RNAlater (Qiagen) using liquid nitrogen and stored at -80°C until RNA extraction. Total RNA was extracted using the RNeasy Mini Kit (Qiagen). The RNA concentration of each sample was adjusted to 0.125 μg/μl and samples were reverse-transcribed using the RT2 HT First Strand cDNA Kit (Qiagen). Custom RT2 Profiler PCR Arrays and Primer Assays (Qiagen) were run with Universal FastStart SYBR Green Master (ROX; Roche) on the StepOne Plus real-time PCR system (Applied Biosystems) using the following cycling conditions: 1) Initial denaturation: 95°C for 14 min; 2) Denaturation: 94°C for 15 sec; 3) Annealing: 61°C for 30 sec; 4) Extension: 72°C for 20 sec. Cycles 2-4 were repeated 40 times. Relative transcript levels were normalized to actin-b. The upper limit of Cq was fixed to 38 cycles. All procedures were performed according to the manufacturer's instructions.

Total gastrointestinal transit time

Total gastrointestinal (GI) transit time was assessed using the carmine red dye assay, which has been described previously [54]. Briefly, carmine red (Sigma-Aldrich) was prepared as a 6% (w/v) solution in 0.5% methylcellulose (Sigma-Aldrich) and autoclaved prior usage. CON mice were kept on the MD, switched to WD 24h before the assay or treated with 100 μl oleic acid 1 hour before and 4 hours after the application of 150 μl carmine red dye. CON mice treated with two times 0.9% saline served as a control for the loperamide treatment. Animals were not fasted beforehand. Feces were collected every 30 min (up to 9 hours from time of gavage) and evaluated for the presence of the carmine red dye. The time from gavage to initial appearance of carmine red in the feces was recorded as the total GI transit time for the respective animal.

Mass spectrometry

Duodenum and cecum content of mice kept on the MD, switched to WD or treated with two doses of 100 μl oleic acid as described previously were collected at 6 h, 9h, 12h or 24h after the switch to WD or treatment with oleic acid. Different gut contents were normalized by weight and suspended in 15 times more (w/v) ultrapure water using device tissue lyser (Qiagen; 3 min 25 Hz). Suspended samples were centrifuged (5 min, full speed) and 70 μl of the supernatant were shock frozen in liquid nitrogen and stored at -80°C. For mass spectrometric analysis, samples were thawed and centrifuged at 20,000 g for 10 min at 4°C. Supernatant was transferred to 96-well storage plates and measured in different dilutions. Relative metabolites levels were quantified with an Agilent 6550 Q-TOF mass spectrometer (Agilent Technologies Inc., Santa Clara, CA) by non-targeted flow injection analysis as described previously [55]. Profile spectra with high mass accuracy were recorded from 50 to 1000 *m/z* in negative ionization mode. The common mass axis after sample alignment was recalibrated using known frequently occurring metabolite ions. Ions were finally annotated based on accurate mass comparison using 1 mDa mass tolerance against a list of compounds derived from the Kegg Database [56] assuming single charged ions after deprotonation.

To quantify cholate (CA) we employed ultra-performance liquid chromatography-high resolution heated electrospray ionization mass spectrometry (UPLC HR HESI-MS). The data were recorded on a Thermo Scientific™ Q Exactive™ Hybrid Quadrupole-Orbitrap

Mass Spectrometer coupled to a Dionex Ultimate 3000 UPLC. According to [57] we used a solvent gradient (A = H_20, 0.1% formic acid, B = acetonitrile, 0.1% formic acid with B at 5% from 0-0.5 min, 5-20% from 0.5-1 min, 20-25% from 1-2 min, 25% from 2-5.5 min, 25-30% from 5.5-6 min, 30% from 6-8 min, 30-35% from 8-9 min, 35-75% from 9-17 min, 75%-100% from 17-18 min and 100% from 18-19 min at a flowrate of 0.5 ml/min) on a Phenomenex Kinetex 2.6 µm XB-C18 100 Å (150 X 4.6 mm) column at 45°C. The MS was operated in negative ionization mode at a scan range of 200-800 *m*/*z* and a resolution of 75000. The spray voltage was set to 3.0 kV, the S-lens to 1, the auxiliary gas heater temperature to 438°C and the capillary temperature to 270°C. Further parameters used were AGC target (1e6), maximum injection time (200 ms), microscans (1), sheath gas (53), aux gas (14) and sweep gas (3). Absolute quantification was achieved by using CA from Sigma-Aldrich as a standard. The standard curve was recorded with water-diluted concentrations of 10 ng/ml, 50 ng/ml, 100 ng/ml, 250 ng/ml, 500 ng/ml, 1 µg/ml, 10 µg/ml and 50 µg/ml from a 1 mg/ml CA stock solution. Data obtained from undiluted sample supernatants were analyzed for CA retention time and ion adduct $[M\text{-}H+HCO_2H]^-$= 453.2857 *m*/*z* with a mass tolerance of 5 ppm. Concentrations were calculated using the Thermo Xcalibur 2.2 Quan Browser.

Flow cytometric analysis of immune cells of the cecal mucosa

Mice were euthanized and the cecum was excised and cut open longitudinally. To dislodge epithelial cells, the cecum tissue was cut into small pieces and incubated twice in 14ml PBS (5 mM EDTA, 15 mM HEPES, 10 % FCS; 20 min; 37 °C; mildly shaking). Subsequently, samples were washed in RPMI (30 % FCS) and transferred to RPMI (1 mg/ml Collagenase VIII (Sigma), 0.2 mg/ml DNase I (Roche)). The tissue pieces were digested mildly shaking for 1 h at 37 °C. The digested tissue was passed through a 70 µm cell strainer and washed with RPMI. The cells were resuspended in RPMI and carefully pipetted onto a NycoPrep (Progen) 1.077 matrix. After centrifugation (30 min, 400 g), cells from the interphase were collected, rinsed with RPMI (15 % FCS) and suspended in PBS (1 % FCS). For intracellular staining, we first performed surface marker staining. Then, cells were fixed and permeabilized for 40 minutes at room temperature in the dark with Foxp3 Fix/Perm buffer (eBioscience/Thermo Fisher). Subsequently, cells were washed with Permeabilization/Wash buffer (eBioscience/Thermo Fisher) and stained for 40 minutes at room temperature in the dark. Antibodies/dyes used in this study: CD45 (30-F11, Biolegend), CD4 (RM4-5, Thermo Fischer), Foxp3 (FJK-16s, Thermo Fischer), F4/80 (BM8, Biolegend), $CD10^3$ (2E7, Biolegend), MHCII (M5/114.15.2, Biolegend), CD11b (M1/70, Biolegend), CD11c (N418, Biolegend), Sytox-blue (Invitrogen), Zombie-NIR (Biolegend).

Flow cytometric analysis of SPI-1 expression using the plasmid pM972

Overnight cultures of *S.*Tm carrying the plasmid pM972 were set up in LB broth containing 50 mg/ml ampicillin and inocula have been prepared as previously described [4]. CON mice were pretreated with ampicillin 24h before infection, switched to WD 24h before infection or treated with 100 µl oleic acid 1 hour before and 4 hours after infection with $5x10^7$ CFU *S.*Tm carrying pM972. Fecal samples were collected 12h, 18h and 24h p.i. and the cecum content was collected 24h p.i. after elimination of the mice. All collected samples were diluted 1:20 (w/v) in sterile PBS. 1 µl of cecum content was stained in 50 µl of PBS

containing anti-O5 rabbit polyclonal antiserum (1:200 v/v) and incubated for 10 min. 200 µl of PBS was added to wash cells. Then, samples were centrifuged (4000 rpm, 20 min) and supernatant was removed. Bacterial cells were suspended in 200 µl PBS. Samples were measured using an LSRII Flow cytometer (Becton Dickenson, NJ, USA) with both forward- and side-scatter parameters at a low, nonzero threshold value and acquired on logarithmic scale. Data were processed using the Flowjo software (Treestar, Ashland, OR, USA).

Flow cytometric assay for measuring cholate-dependent killing

*S.*Tm wt strain and the mutant strains Δ*tolC* and Δ*acrB* were grown overnight at 37°C shaking (160 rpm) in LB broth containing the appropriate antibiotics. Ileum, cecum and colon content of untreated CON mice was collected and diluted 1:20 (w/v) in sterile M9 base salts. Different concentrations (0.125%, 0.5%, 1%, 2% and 8%) of cholate were dissolved in M9 base salts. M9 base salts alone served as a control for potential killing of the gut microbiota upon oxygen contact. 100 µl of M9 base salts only or the respective cholate solutions were pipetted into a 96-well plate, mixed with 1 µl of the different gut contents (harboring microbiota) or the three *S.*Tm strains and incubated for 20 min at room temperature. Afterwards, samples were centrifuged (4000 rpm, 20 min), supernatant was removed and bacterial cells were suspended in 200 µl PBS containing SYTOXgreen (1:5000 v/v; Invitrogen, ThermoFisher) to detect bacteria with loss of membrane integrity. This dye can only penetrate to stain the DNA of microbes when the cell membrane is compromised. The SYTOX-positive ($SYTOX^+$) fraction was quantified by LSRII Flow cytometer (Becton Dickenson, NJ, USA) with both forward- and side-scatter parameters at a low, non-zero threshold value and acquired on logarithmic scale. Data were processed using the Flowjo software (Treestar, Ashland, OR, USA).

Minimal inhibitory concentration assay

The sensitivity of *S.*Tm wt, the mutants deficient in the AcrAB-TolC and AcrAD-TolC efflux pump against certain antimicrobials and primary bile salts was assessed using the minimal inhibitory concentration (MIC) assay, which has been described previously [58]. Briefly, overnight cultures of the different strains were adjusted to an OD_{600} of 1 and further diluted 1:2000 in LB broth to obtain 10^4 CFU per well (assay was performed in sterile 96-well plates). Stock solutions of the different antimicrobial agents have been generated in LB broth as the following: 0.0625 µg/ml ciprofloxacin, 100 µg/ml rifampicin, 100 µg/ml erythromycin, 6.25 µg/ml tetracycline, 10 µg/ml polymyxin B, 8% cholate and 8% taurocholate. Each stock was further serially diluted 1:2 and 50 µl of the different antimicrobial agent solutions were mixed with 50 µl of the respective inocula. The plates were incubated at 37°C and growth was measured at 0 hours, 4 hours, 6 hours, 8 hours and 24h by measuring the OD_{600} with the Spectramax plus (Bucher Biotec). During the incubation between 8 hours and 24h of growth, plates were sealed with Breathe-easierTM tape (Sigma-Aldrich) and covered with the lid of the 96-well plates. The function $y = A + Ce^{-e^{B(x-M)}}$ was fit to the OD600 values dependent on the log10 of the drug concentration [59]. The MIC was then calculated as the drug concentration where the line y=A (the lower asymptote of y) intersects with the line tangential at x=M. The 50% MIC was calculated as the drug concentration where the same line tangential intersects with the line y=0.5*(C-A), the y-value where growth is half-maximal. 95% and 5% confidence intervals were calculated

by adding and subtracting the standard error of the fit multiplied by the 95% entry of the student-t statistic for 32 degrees of freedom to and from the value of the fit at y=0.5*(C-A), respectively.

Determination of cholate sensitivity across individual microbiota strains

Experiments were performed under anoxic conditions (2% H_2, 12% CO_2 in N_2) in an anaerobic chamber (Coy Laboratory Products Inc) using pre-reduced modified Gifu Anaerobic Broth (MGAM, HyServe GmbH, Germany) at 37°C. Strains were grown twice overnight before recording growth curves. Bacterial growth in the presence of the indicated concentrations of sodium cholate or taurocholate (Sigma Aldrich) was monitored in NUNC 96-well U bottom plates (Fisher Scientific) using a starting optical density (OD) at 578nm of 0.01 for all strains. Plates were sealed with breathable membranes (Breathe-Easy®) and incubated at 37°C without shaking. OD578 was measured every hour for 24 hours after 30 seconds of linear shaking with a microplate spectrophotometer (EON, Biotek) by a microplate stacker (Biostack 4, Biotek). Time points with sudden spikes in OD (e.g. caused by condensation) were removed. All plates contained medium-only control wells to allow comparison to unperturbed growth. For each strain, control growth curves were used to determine the time of transition from exponential to stationary phase and all growth curves were truncated using this time point. To quantify growth, we calculated the area under the curve (AUC) using the trapezoidal rule. For baseline correction, we assumed a constant shift and subtracted the same shift to all time points of the growth curves such that the starting OD was zero. AUCs were normalized by dividing the AUC for specific cholate concentrations by the mean AUC of unperturbed growth of the same strain within the same plate. Mean normalized AUCs from three biological replicates are shown.

Mathematical modeling

In order to understand how sensitivities of *S.*Tm and the microbiota to an increase in bile concentration will change the ability of *S.*Tm to establish a transiently stable population in the mouse intestine, we devised a simple mathematical model. In the following, we will introduce the different parameters of the model, and explain how they were derived from our own measurements or from published data (see also table S6 for a list of all parameters).

Dependence of bacterial growth on bile salt concentrations—We used the data describing the effect of different cholate concentrations on growth of the different microbes (figure 2e and figure S13) to infer a mathematical relationship between bile concentration and bacterial growth, both for *S.*Tm and the murine microbiota. In order to do this, we performed linear regression on the natural logarithm of the normalized AUC values, in the concentration range between 0% and 1% cholate (figure S13), separately for the bacterial species tested. The slope of these regression lines is the rate parameter for the exponential decay of growth rate with bile salt concentration. Importantly, this way to estimate dependence of growth on cholate is independent of the differences in growth yields and lag times between strains. Owing to the nature of the measurement of AUC (see above), this estimation of growth assumes that all strains start growing exponentially after the lag time of the 0% sample of a given strain (which is reasonable given our data), and the measurement stops at the time when the 0% sample reaches saturation. The rate of growth between these

two time points is then described by a single exponential function, effectively averaging over potential growth transitions that happen during this time (figure S14).

In order to get a value for the overall growth dependence of the microbiota (as opposed to the single microbiota members) on cholate concentration, we simply took the unweighted average of the slope of all members of the murine microbiota. Note that this is a crude way of assuming the true value, as taking the unweighted average assumes equal numbers of all bacteria in the microbiota, which is an oversimplification.

With this, we have parameters for the rate of decrease in growth rate with bile salt concentration, for both *S.*Tm and the murine microbiota (w/o *E. coli*). We denote these rates as k_S and k_M, respectively. We can now formulate expressions for the growth rates of *S.*Tm and the microbiota, r_S and r_M, depending on the bile saltconcentration,

$$r_S = r_{S,max} * e^{-k_S * BA}$$

$$r_M = r_{M,max} * e^{-k_M * BA}$$

where $r_{S,max}$ and $r_{M,max}$ are the maximum growth rates of *S.*Tm and the microbiota (i.e., the growth rates at $BA = 0$), respectively. Maximum growth rates were set to 1.1 h^{-1} for both the microbiota and *S.*Tm. This is based on measured data for both *S.*Tm (measured growth rate is 1.10 h^{-1}) and *Bacteroides thetaiotaomicron* (measured growth rate 1.05 h^{-1} [60]).

Estimation of the initial population sizes—To estimate the initial *S.*Tm^{wt} and *S.*Tm^{acrAB} (mutant with nonfunctional AcrAB/TolC efflux pump) population size S, we used the experimental inoculum size used for the infections, $S = 5 * 10^7$. The microbiota population size without bile salt is set to be 10^{11} cells [61], and the results shown in figure 3a,b are generated using $M = 10^{11}$ consistently.

It is of interest that this number reflects a steady state of microbiota growth and loss through outflow. Inhibition of growth by bile salt, assuming outflow to be unchanged, could therefore lead to a decrease in microbiota population size that is directly proportional to microbiota growth, and can thus be modeled using the same kinetics (see previous paragraph for the estimation of parameters),

$$M(BA) = 10^{11} * e^{-kM * BA}.$$

We tested how adding this dependence of the initial microbiota population size on bile concentrations to the model changes the outcome, and show the results below (see section "Model results").

Population dynamics—To describe the population dynamics of *S.*Tm and the microbiota, we now formulate the following differential equations, where S denotes *S.*Tm population size, and M the microbiota population size:

$$\frac{dS}{dt} = S * \left(r_S - (S + M) * d\right)$$

$$\frac{dM}{dt} = M * \left(r_M - (S + M) * d\right)$$

where d is a description of clearance and death, introducing an effective carrying capacity for the total population size of $(S + M)$, which dynamically relates the two populations.

Model results—The results for the modeled competition of *S.*Tm^{WT} and *S.*Tm^{acrAB} strains against the murine microbiota after 24h with constant initial microbiota population sizes are depicted in figure 3A,B in the main text.

In figure S15, we show in addition how changing initial microbiota population size in response to bile (see section "Estimation of initial population sizes") affects the results of this competition. This modification of the model leads to increasingly smaller M with increasing bile salt concentrations. In the case of competition of *S.*Tm^{WT} against the microbiota, this only leads to small quantitative differences in realistic bile salt concentrations (i.e., below 1%, figure S15a) when compared to the model with constant initial microbiota population size (figure 3a,b). However, in the case of competition of *S.*Tm^{acrAB} strain against the microbiota (figure S15b), we observe a qualitative difference in the observed curves when comparing to the model with constant initial microbiota population size: at high bile salt concentrations, the *S.*Tm^{acrAB} population increases (figure S15b, cyan line). There is a simple explanation for this: very little growth happens in either population at these bile salt concentrations, and the observed population sizes are therefore largely determined by the initial population size; as the initial microbiota population size gets smaller with increasing bile salt concentration, but the initial *S.*Tm^{acrAB} population size remains constant, we observe the behavior shown in figure S15b.

Numerical simulations—To solve the system numerically, we used the function ode in the package deSolve [62] in the R language of statistical computing [63]. The time resolution of the simulations is 12min.

Sequence analysis of *arcAB*-and *tolC*-like genes

The *Salmonella* protein sequences were queried against the full proteome sequences of the other 27 tested strains by BLASTp. Targets with an alignment bitscore of at least 60 were considered as homologs of *acrAB/tolC*. Phylogenetic relationship, cholate resistance (data represent average AUC values from figure 2e) and bitscores were visualized using iTOL v3 [64].

Statistical Analysis

Sample size was determined from data of previous studies. Scientists were not blinded for the assignment of the experiments and the data analysis. The exact Mann-Whitney U test was performed when two groups were compared. The one-way ANOVA was carried out when two or more treatment groups were compared. When time courses/different sampling sides were compared with two or more groups, Two-way ANOVA was used to determine significance. The statistical analysis was performed by the software Graphpad Prism Version 7.02 for Windows (GraphPad Software). P-values of less than 0.05 were considered to indicate statistical significance. C.I.s to C.I. of the inoculum were compared using ratios of strain 1 and strain 2 in comparison to the ratio of both strains in the inoculum.

Supplementary Material

Refer to Web version on PubMed Central for supplementary material.

Acknowledgement

We are grateful to the members of the Hardt lab and to Roman Stocker for helpful scientific discussions. The RCHCI staff (especially Katharina Holzinger, Dennis Mollenhauer & Sven Nowok) for excellent support of our animal work is gratefully acknowledged. The authors have no conflicting financial interests. E.S. is supported by the Swiss National Science Foundation (SNF, Marie Heim-Vögtlin award PMPDP3_158364 and Ambizione award PZ00P3_136742) and the Gebert Rüf "Microbials" programme (GRS-073/17). W.-D. H. is supported by the SNF (310030_153074 and 310030B_173338/1; Sinergia CRSII_154414/1; NRP 72 407240-167121), ETH Zurich (ETH-33 12-2) the Novartis Freenovation Programme and the Promedica Foundation, Chur. S.S. is supported by ETH Zurich and the Helmut Horten Foundation. E.B. is supported by a Boehringer Ingelheim Fonds PhD Stipend and E.G. by a grant from the Monique Dornonville de la Cour Foundation. B.S. is supported by the German Research Foundation (STE 1971/4-2 SPP 1656/2) and the German Center for Infection Research (DZIF).

References

1. Stecher B, Berry D, Loy A. Colonization resistance and microbial ecophysiology: using gnotobiotic mouse models and single-cell technology to explore the intestinal jungle. FEMS microbiology reviews. 2013; 37:793–829. DOI: 10.1111/1574-6976.12024 [PubMed: 23662775]
2. David LA, et al. Diet rapidly and reproducibly alters the human gut microbiome. Nature. 2014; 505:559–563. DOI: 10.1038/nature12820 [PubMed: 24336217]
3. Desai MS, et al. A Dietary Fiber-Deprived Gut Microbiota Degrades the Colonic Mucus Barrier and Enhances Pathogen Susceptibility. Cell. 2016; 167:1339–1353 e1321. DOI: 10.1016/j.cell.2016.10.043 [PubMed: 27863247]
4. Barthel M, et al. Pretreatment of mice with streptomycin provides a Salmonella enterica serovar Typhimurium colitis model that allows analysis of both pathogen and host. Infect Immun. 2003; 71:2839–2858. [PubMed: 12704158]
5. Brugiroux S, et al. Genome-guided design of a defined mouse microbiota that confers colonization resistance against Salmonella enterica serovar Typhimurium. Nat Microbiol. 2016; 2doi: 10.1038/nmicrobiol.2016.215
6. Stecher B, et al. Gut inflammation can boost horizontal gene transfer between pathogenic and commensal Enterobacteriaceae. Proc Natl Acad Sci U S A. 2012; 109:1269–1274. DOI: 10.1073/pnas.1113246109 [PubMed: 22232693]
7. Arkan MC, et al. IKK-beta links inflammation to obesity-induced insulin resistance. Nat Med. 2005; 11:191–198. DOI: 10.1038/nm1185 [PubMed: 15685170]
8. Kim KA, Gu W, Lee IA, Joh EH, Kim DH. High fat diet-induced gut microbiota exacerbates inflammation and obesity in mice via the TLR4 signaling pathway. PLoS One. 2012; 7:e47713.doi: 10.1371/journal.pone.0047713 [PubMed: 23091640]

9. Moya-Perez A, Neef A, Sanz Y. Bifidobacterium pseudocatenulatum CECT 7765 Reduces Obesity-Associated Inflammation by Restoring the Lymphocyte-Macrophage Balance and Gut Microbiota Structure in High-Fat Diet-Fed Mice. PLoS One. 2015; 10:e0126976.doi: 10.1371/journal.pone.0126976 [PubMed: 26161548]
10. Hwang DH, Kim JA, Lee JY. Mechanisms for the activation of Toll-like receptor 2/4 by saturated fatty acids and inhibition by docosahexaenoic acid. Eur J Pharmacol. 2016; 785:24–35. DOI: 10.1016/j.ejphar.2016.04.024 [PubMed: 27085899]
11. Stecher B, Maier L, Hardt WD. 'Blooming' in the gut: how dysbiosis might contribute to pathogen evolution. Nat Rev Microbiol. 2013; 11:277–284. DOI: 10.1038/nrmicro2989 [PubMed: 23474681]
12. Reddy BS, Mangat S, Sheinfil A, Weisburger JH, Wynder EL. Effect of type and amount of dietary fat and 1,2-dimethylhydrazine on biliary bile acids, fecal bile acids, and neutral sterols in rats. Cancer Res. 1977; 37:2132–2137. [PubMed: 861940]
13. Reddy BS. Diet and excretion of bile acids. Cancer Res. 1981; 41:3766–3768. [PubMed: 6266664]
14. Cummings JH, et al. Influence of diets high and low in animal fat on bowel habit, gastrointestinal transit time, fecal microflora, bile acid, and fat excretion. J Clin Invest. 1978; 61:953–963. DOI: 10.1172/JCI109020 [PubMed: 659584]
15. Begley M, Gahan CG, Hill C. The interaction between bacteria and bile. FEMS Microbiol Rev. 2005; 29:625–651. DOI: 10.1016/j.femsre.2004.09.003 [PubMed: 16102595]
16. Islam KB, et al. Bile acid is a host factor that regulates the composition of the cecal microbiota in rats. Gastroenterology. 2011; 141:1773–1781. DOI: 10.1053/j.gastro.2011.07.046 [PubMed: 21839040]
17. Urdaneta V, Casadesus J. Interactions between Bacteria and Bile Salts in the Gastrointestinal and Hepatobiliary Tracts. Front Med (Lausanne). 2017; 4:163.doi: 10.3389/fmed.2017.00163 [PubMed: 29043249]
18. MacConkey AT. Bile Salt Media and their advantages in some Bacteriological Examinations. J Hyg (Lond). 1908; 8:322–334. [PubMed: 20474363]
19. Buckley AM, et al. The AcrAB-TolC efflux system of Salmonella enterica serovar Typhimurium plays a role in pathogenesis. Cell Microbiol. 2006; 8:847–856. DOI: 10.1111/j.1462-5822.2005.00671.x [PubMed: 16611233]
20. Nishino K, Latifi T, Groisman EA. Virulence and drug resistance roles of multidrug efflux systems of Salmonella enterica serovar Typhimurium. Mol Microbiol. 2006; 59:126–141. DOI: 10.1111/j.1365-2958.2005.04940.x [PubMed: 16359323]
21. Devkota S, et al. Dietary-fat-induced taurocholic acid promotes pathobiont expansion and colitis in Il10-/- mice. Nature. 2012; 487:104–108. DOI: 10.1038/nature11225 [PubMed: 22722865]
22. Stecher B, et al. Salmonella enterica serovar typhimurium exploits inflammation to compete with the intestinal microbiota. PLoS Biol. 2007; 5:2177–2189. DOI: 10.1371/journal.pbio.0050244 [PubMed: 17760501]
23. Winter SE, et al. Gut inflammation provides a respiratory electron acceptor for Salmonella. Nature. 2010; 467:426–429. DOI: 10.1038/nature09415 [PubMed: 20864996]
24. Winter SE, et al. Host-derived nitrate boosts growth of E. coli in the inflamed gut. Science. 2013; 339:708–711. DOI: 10.1126/science.1232467 [PubMed: 23393266]
25. Raffatellu M, et al. Lipocalin-2 resistance confers an advantage to Salmonella enterica serotype Typhimurium for growth and survival in the inflamed intestine. Cell Host Microbe. 2009; 5:476–486. DOI: 10.1016/j.chom.2009.03.011 [PubMed: 19454351]
26. Litvak Y, Byndloss MX, Baumler AJ. Colonocyte metabolism shapes the gut microbiota. Science. 2018; 362doi: 10.1126/science.aat9076
27. Miki T, Goto R, Fujimoto M, Okada N, Hardt WD. The Bactericidal Lectin RegIIIbeta Prolongs Gut Colonization and Enteropathy in the Streptomycin Mouse Model for Salmonella Diarrhea. Cell Host Microbe. 2017; 21:195–207. DOI: 10.1016/j.chom.2016.12.008 [PubMed: 28111202]
28. Miki T, Holst O, Hardt WD. The bactericidal activity of the C-type lectin RegIIIbeta against Gram-negative bacteria involves binding to lipid A. J Biol Chem. 2012; 287:34844–34855. DOI: 10.1074/jbc.M112.399998 [PubMed: 22896700]

29. Mukherjee S, et al. Antibacterial membrane attack by a pore-forming intestinal C-type lectin. Nature. 2014; 505:103–107. DOI: 10.1038/nature12729 [PubMed: 24256734]
30. Lopez CA, et al. Phage-mediated acquisition of a type III secreted effector protein boosts growth of salmonella by nitrate respiration. mBio. 2012; 3doi: 10.1128/mBio.00143-12
31. Berg RD. The indigenous gastrointestinal microflora. Trends Microbiol. 1996; 4:430–435. [PubMed: 8950812]
32. Piddock LJ. Multidrug-resistance efflux pumps - not just for resistance. Nat Rev Microbiol. 2006; 4:629–636. DOI: 10.1038/nrmicro1464 [PubMed: 16845433]
33. Wotzka SY, et al. Microbiota stability in healthy individuals after single-dose lactulose challenge-A randomized controlled study. PLoS One. 2018; 13:e0206214.doi: 10.1371/journal.pone.0206214 [PubMed: 30359438]
34. Litvak Y, et al. Commensal Enterobacteriaceae Protect against Salmonella Colonization through Oxygen Competition. Cell Host Microbe. 2019; 25:128–139 e125. DOI: 10.1016/j.chom.2018.12.003 [PubMed: 30629913]
35. Sana TG, et al. Salmonella Typhimurium utilizes a T6SS-mediated antibacterial weapon to establish in the host gut. Proc Natl Acad Sci U S A. 2016; 113:E5044–5051. DOI: 10.1073/pnas.1608858113 [PubMed: 27503894]
36. Deriu E, et al. Probiotic bacteria reduce salmonella typhimurium intestinal colonization by competing for iron. Cell Host Microbe. 2013; 14:26–37. DOI: 10.1016/j.chom.2013.06.007 [PubMed: 23870311]
37. Nedialkova LP, et al. Temperate phages promote colicin-dependent fitness of Salmonella enterica serovar Typhimurium. Environ Microbiol. 2016; 18:1591–1603. DOI: 10.1111/1462-2920.13077 [PubMed: 26439675]
38. Conway T, Cohen PS. Commensal and Pathogenic Escherichia coli Metabolism in the Gut. Microbiol Spectr. 2015; 3doi: 10.1128/microbiolspec.MBP-0006-2014
39. Baucheron S, et al. AcrAB-TolC directs efflux-mediated multidrug resistance in Salmonella enterica serovar typhimurium DT104. Antimicrob Agents Chemother. 2004; 48:3729–3735. DOI: 10.1128/AAC.48.10.3729-3735.2004 [PubMed: 15388427]
40. Eaves DJ, Ricci V, Piddock LJ. Expression of acrB, acrF, acrD, marA, and soxS in Salmonella enterica serovar Typhimurium: role in multiple antibiotic resistance. Antimicrob Agents Chemother. 2004; 48:1145–1150. [PubMed: 15047514]
41. Urdaneta V, Casadesus J. Adaptation of Salmonella enterica to bile: essential role of AcrAB-mediated efflux. Environ Microbiol. 2018; doi: 10.1111/1462-2920.14047
42. Theriot CM, et al. Antibiotic-induced shifts in the mouse gut microbiome and metabolome increase susceptibility to Clostridium difficile infection. Nature communications. 2014; 5doi: 10.1038/ncomms4114
43. Rozwandowicz M, et al. Plasmids carrying antimicrobial resistance genes in Enterobacteriaceae. J Antimicrob Chemother. 2018; 73:1121–1137. DOI: 10.1093/jac/dkx488 [PubMed: 29370371]
44. Hoiseth SK, Stocker BA. Aromatic-dependent Salmonella typhimurium are non-virulent and effective as live vaccines. Nature. 1981; 291:238–239. [PubMed: 7015147]
45. Datsenko KA, Wanner BL. One-step inactivation of chromosomal genes in Escherichia coli K-12 using PCR products. Proc Natl Acad Sci U S A. 2000; 97:6640–6645. DOI: 10.1073/pnas.120163297 [PubMed: 10829079]
46. Grant AJ, et al. Modelling within-host spatiotemporal dynamics of invasive bacterial disease. PLoS Biol. 2008; 6:e74.doi: 10.1371/journal.pbio.0060074 [PubMed: 18399718]
47. Gil D, Bouche JP. ColE1-type vectors with fully repressible replication. Gene. 1991; 105:17–22. [PubMed: 1937005]
48. Kaiser P, et al. Cecum lymph node dendritic cells harbor slow-growing bacteria phenotypically tolerant to antibiotic treatment. PLoS Biol. 2014; 12:e1001793.doi: 10.1371/journal.pbio.1001793 [PubMed: 24558351]
49. Moor K, et al. High-avidity IgA protects the intestine by enchaining growing bacteria. Nature. 2017; 544:498–502. DOI: 10.1038/nature22058 [PubMed: 28405025]

50. Sturm A, et al. The cost of virulence: retarded growth of Salmonella Typhimurium cells expressing type III secretion system 1. PLoS Pathog. 2011; 7:e1002143.doi: 10.1371/journal.ppat.1002143 [PubMed: 21829349]
51. Li H, et al. The outer mucus layer hosts a distinct intestinal microbial niche. Nat Commun. 2015; 6doi: 10.1038/ncomms9292
52. Apprill A, McNally S, Parsons R, Weber L. Minor revision to V4 region SSU rRNA 806R gene primer greatly increases detection of SAR11 bacterioplankton. AQUATIC MICROBIAL ECOLOGY. 2015; 75:129–137. DOI: 10.3354/ame01753
53. Parada AE, Needham DM, Fuhrman JA. Every base matters: assessing small subunit rRNA primers for marine microbiomes with mock communities, time series and global field samples. Environ Microbiol. 2016; 18:1403–1414. DOI: 10.1111/1462-2920.13023 [PubMed: 26271760]
54. Dey N, et al. Regulators of gut motility revealed by a gnotobiotic model of diet-microbiome interactions related to travel. Cell. 2015; 163:95–107. DOI: 10.1016/j.cell.2015.08.059 [PubMed: 26406373]
55. Fuhrer T, Heer D, Begemann B, Zamboni N. High-throughput, accurate mass metabolome profiling of cellular extracts by flow injection-time-of-flight mass spectrometry. Anal Chem. 2011; 83:7074–7080. DOI: 10.1021/ac201267k [PubMed: 21830798]
56. Kanehisa M, Goto S. KEGG: kyoto encyclopedia of genes and genomes. Nucleic Acids Res. 2000; 28:27–30. [PubMed: 10592173]
57. Yin S, et al. Factors affecting separation and detection of bile acids by liquid chromatography coupled with mass spectrometry in negative mode. Anal Bioanal Chem. 2017; 409:5533–5545. DOI: 10.1007/s00216-017-0489-1 [PubMed: 28689325]
58. Wiegand I, Hilpert K, Hancock RE. Agar and broth dilution methods to determine the minimal inhibitory concentration (MIC) of antimicrobial substances. Nat Protoc. 2008; 3:163–175. DOI: 10.1038/nprot.2007.521 [PubMed: 18274517]
59. Lambert RJ, Pearson J. Susceptibility testing: accurate and reproducible minimum inhibitory concentration (MIC) and non-inhibitory concentration (NIC) values. J Appl Microbiol. 2000; 88:784–790. [PubMed: 10792538]
60. Cremer J, Arnoldini M, Hwa T. Effect of water flow and chemical environment on microbiota growth and composition in the human colon. Proc Natl Acad Sci U S A. 2017; 114:6438–6443. DOI: 10.1073/pnas.1619598114 [PubMed: 28588144]
61. Vandeputte D, et al. Quantitative microbiome profiling links gut community variation to microbial load. Nature. 2017; 551:507–511. DOI: 10.1038/nature24460 [PubMed: 29143816]
62. Soetaert K, Petzoldt T, Setzer RW. Solving Differential Equations in R: Package deSolve. J Stat Softw. 2010; 33:1–25. [PubMed: 20808728]
63. Team, R. C. (2014)
64. Letunic I, Bork P. Interactive tree of life (iTOL) v3: an online tool for the display and annotation of phylogenetic and other trees. Nucleic Acids Res. 2016; 44:W242–245. DOI: 10.1093/nar/gkw290 [PubMed: 27095192]

Europe PMC Funders Author Manuscripts

Europe PMC Funders Author Manuscripts

One sentence Summary

Dietary fat can promote enterobacteriaceal blooms in mice.

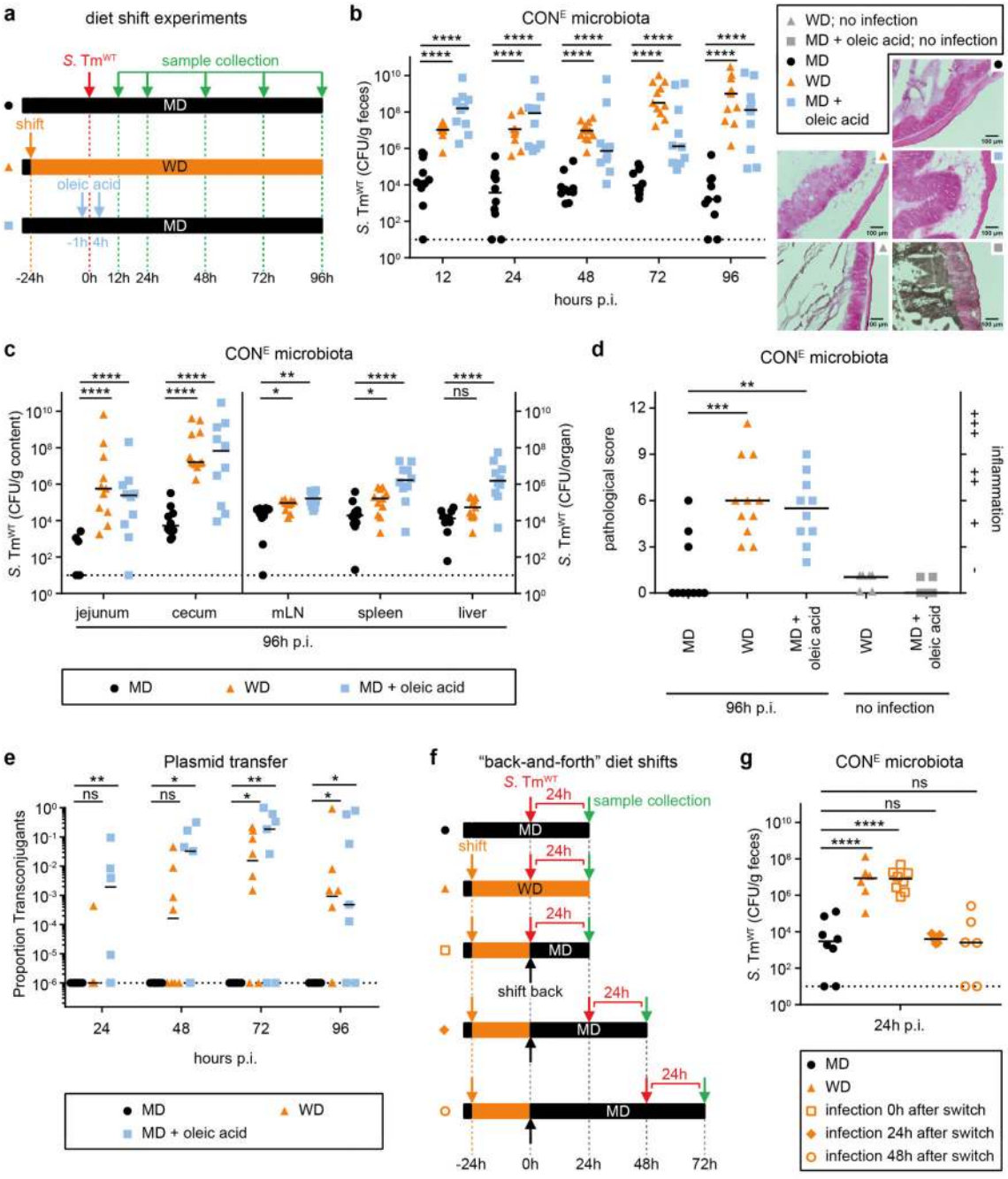

Figure 1. A shift to WD and oleic acid gavage promote *S.*Tm blooms, enteropathy and plasmid transfer.

(a) Experimental protocol. (b-d) Pathogen loads and cecum tissue histopathology of CON^E mice infected with 5x10^7 CFU *S.*Tm by gavage (N=6,10,11). Non-infected controls 96h after diet-shift or oleic acid gavage (grey symbols; N=6; no CFU detected). See 'Histological procedures' in Methods for details of pathological score. H&E images represent median sample from corresponding treatment. (e) *In vivo* transconjugation was determined by stool plating (N=7,8; Kruskal-Wallis test, multiple comparison correction; see figure S6). (f) Protocol of back-and-forth diet-shifts in CON^E mice. (g) Fecal pathogen loads were

Europe PMC Funders Author Manuscripts

analyzed 24h p.i. with $5x10^7$ CFU *S.*Tm (by gavage; N=5,6,8,9 mice). Bars: median; Two-way ANOVA on log-normalized data with Dunnett's multiple comparison test (for b,c,g), two-tailed Mann-Whitney-U (for d). Dotted lines = detection limit. ns, not significant ($p > 0.05$), *$p < 0.05$, **$p < 0.01$, ***$p < 0.005$, ****$p < 0.001$. MD: maintenance diet, WD: Western-type diet.

Europe PMC Funders Author Manuscripts

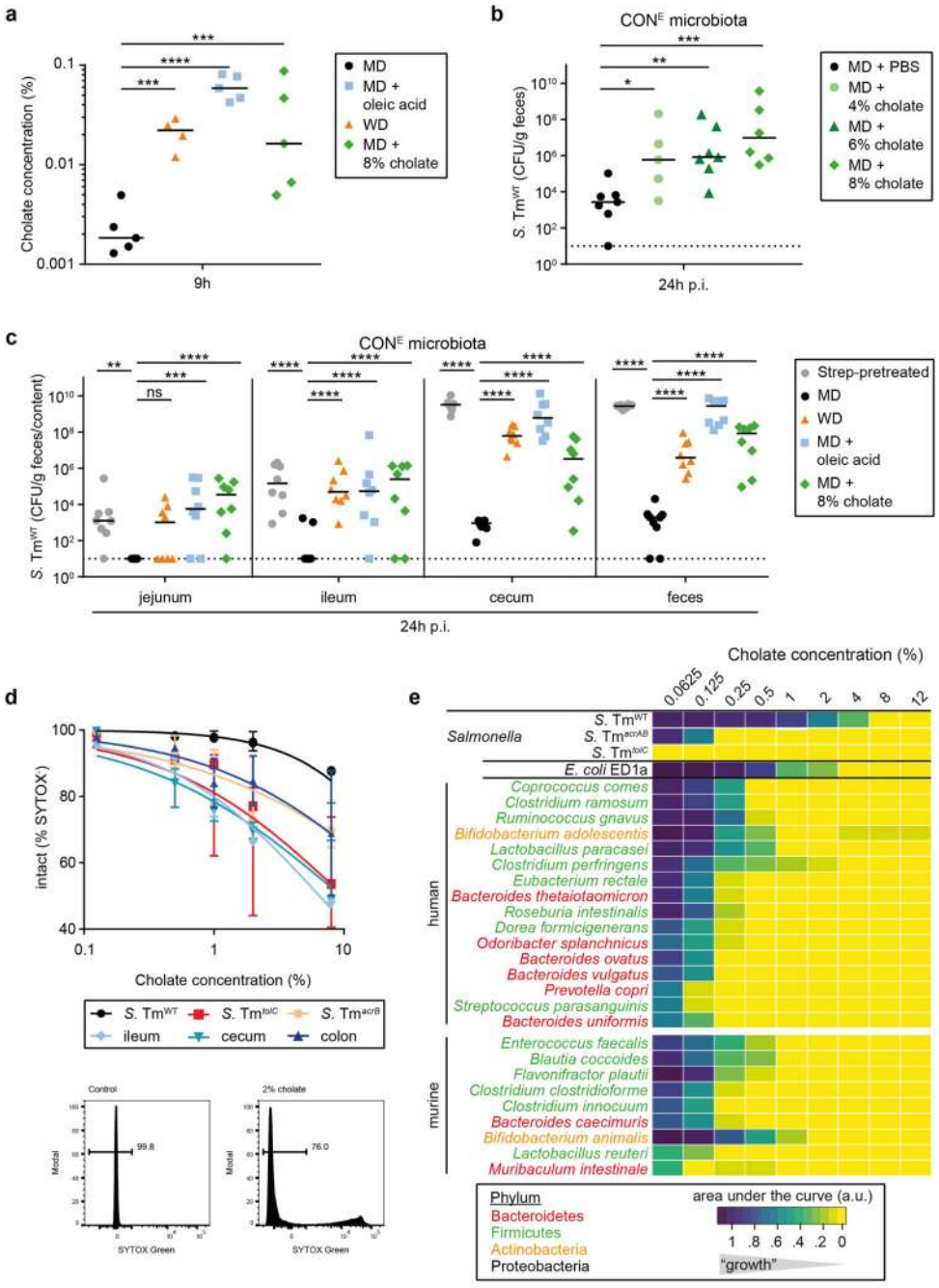

Figure 2. Primary bile salts can explain *S.*Tm blooms.

(a) Quantitative cholate mass spectrometry analysis in CON^{E} mice (N=5) 9h after the indicated intervention. (b) Cholate titration experiment. CON^{E} mice (N=5,6,7) were gavaged as indicated (100µl) 1h before and 4h after *S.*Tm infection (5x10^{7} CFU). (c) Effect of the indicated interventions on gut luminal *S.*Tm densities (N=8,9). Control: CON^{E} mice pre-treated with streptomycin (20 mg by gavage; 24h before infection; grey). (d) Cholate sensitivity of gut-luminal microbiota from ileum (N=2), cecum (N=3) and colon (N=2) microbiota (isolated from CON^{E} mice) and of wt *S.*Tm (black circles; N=3) or indicated

Europe PMC Funders Author Manuscripts

*S.*Tm mutants (N=3). Analysis was performed by SYTOXgreen-exclusion and flow cytometry (exemplary gating for *S.* Tm^{tolC} is shown). The mean value of all experiments is shown (whiskers = range). (e) Cholate-sensitivity of individual microbiota strains as analyzed in MGAM medium (2% H2, 12% CO_2, 86% N_2; table S3; N=3, analysis vs. growth without inhibitor). Controls: Wt *E. coli* ED1a, indicated *S.*Tm strains. Bars: median; Two-way ANOVA on log-normalized data with Dunnett's multiple comparison test. Dotted lines = detection limit. ns, not significant ($p > 0.05$), *$p < 0.05$, **$p < 0.01$, ***$p < 0.005$, ****$p < 0.001$.

Europe PMC Funders Author Manuscripts

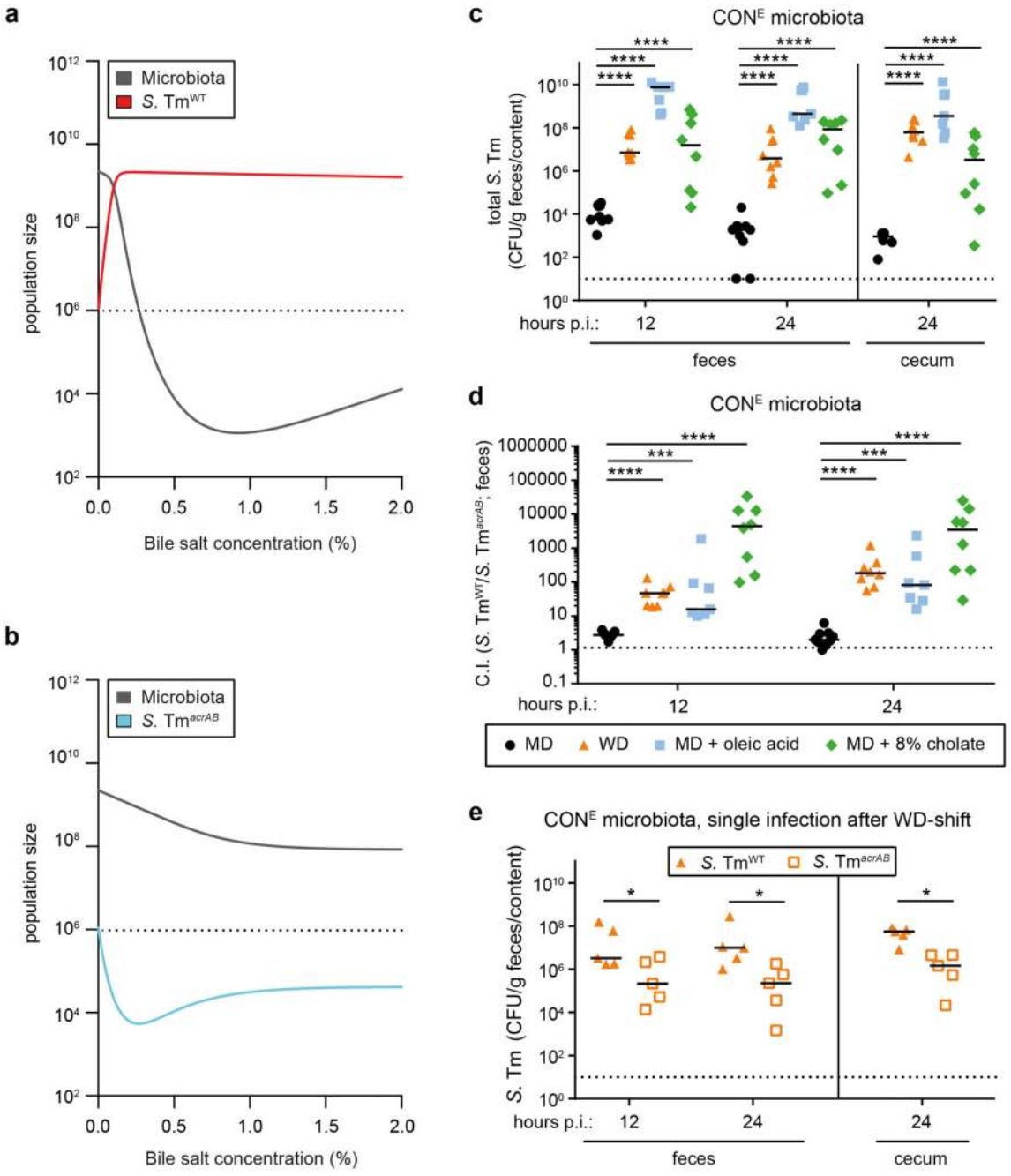

Figure 3. Modeling and experimental data validate that bile-resistance promotes *S*.Tm growth in the fat-exposed gut.

(a,b) Mathematical model testing if bile-mediated growth inhibition can explain *S*.Tm vs. *S*.Tm^{arcAB} blooms after 24h of growth in the fat-, oleic acid- or cholate exposed gut (as detailed in Supplementary Information). (c,d) Competitive infections. CON^{E} mice (N=7,8,9) were treated as above and infected with *S*.Tm^{wt} and *S*.Tm^{acrAB} (1:1; 5x10^{7} CFU total, by gavage). *S*.Tm loads were quantified by plating. (d) The competitive index of *S*.Tm^{wt} vs. *S*.Tm^{acrAB} as analysed by WITS-qPCR. (e) Total *S*.Tm^{wt} or *S*.Tm^{acrAB} loads in CON^{E} mice (C57BL/6, N=5) infected as in figure 1a and analysed by plating 24h p.i. Bars: median;

Europe PMC Funders Author Manuscripts

Two-way ANOVA on log-normalized data with Dunnett's multiple comparison test. Dotted lines = detection limit. *p<0.05, **p<0.01, ***p<0.005, ****p<0.001.

Europe PMC Funders Author Manuscripts

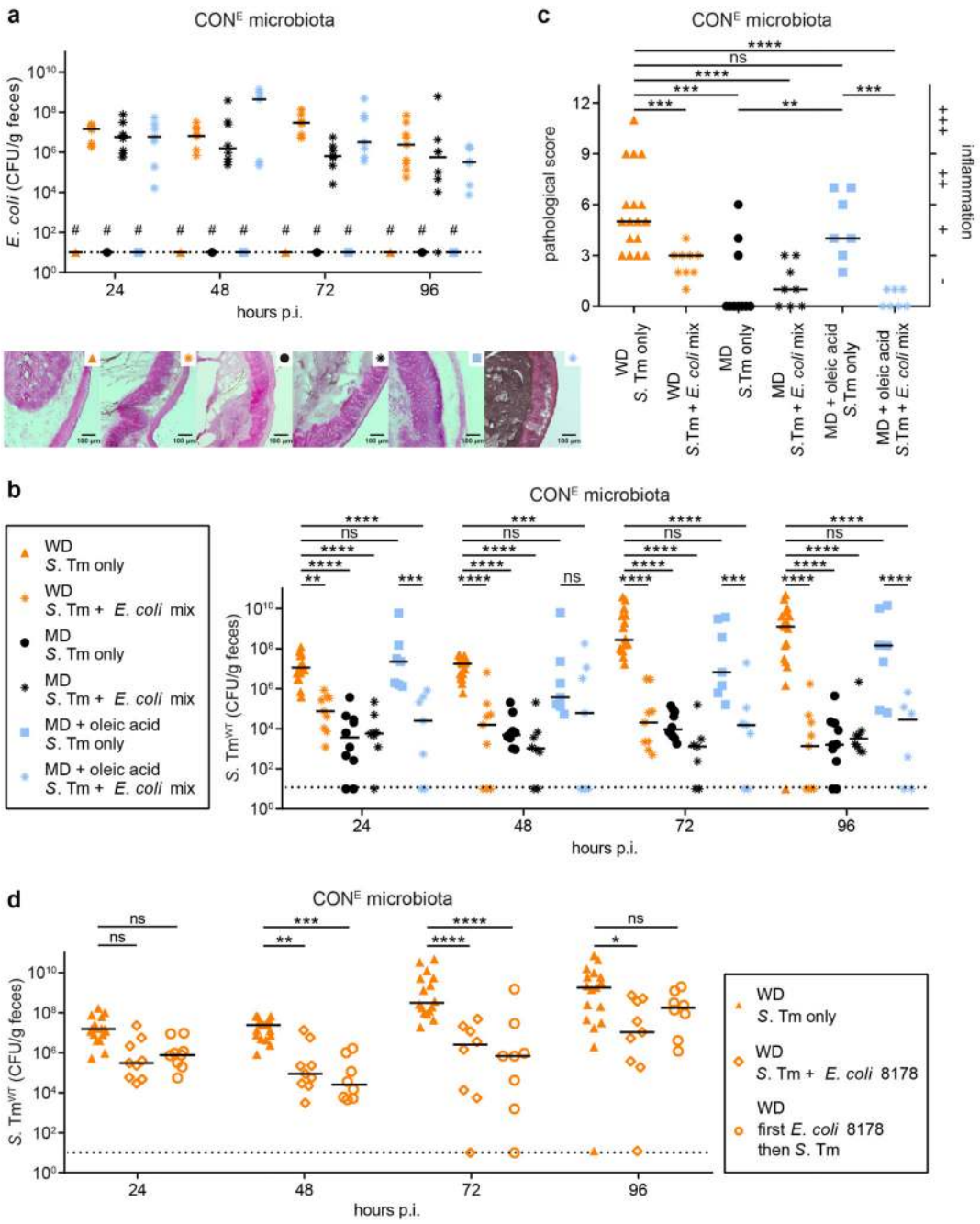

Figure 4. *E. coli* limits the *S*.Tm infection after WD-shift or oleic acid gavage.

(a-c) Competitive infection with the *E. coli* mix. CON^E mice (N=7,8,9,10,17) were treated as in figure 1a and infected with wt *S*.Tm and the *E. coli* 8178, CFT073 and Z1324 mix, as indicated (5x10^7 CFU by gavage). (a,b) *E. coli* and *S*.Tm loads were determined by plating. (c) Cecum histopathology 96h p.i.. H&E images represent median sample from corresponding treatment. (d) Competitive infection with *E. coli* 8178. CON^E mice (N=9,15) were treated as above and gavaged with *E. coli* 8178 and *S*.Tm, as indicated (5x10^7 cfu). Triangles: control mice re-plotted from (b). #: none detected; Bars: median; ns, not

Europe PMC Funders Author Manuscripts

significant ($p > 0.05$), *$p < 0.05$, **$p < 0.01$, ***$p < 0.005$, ****$p < 0.001$, Two-way ANOVA on log-normalized data with Dunnett's multiple comparison test (for b,d), two-tailed Mann-Whitney U-test (for c). Dotted lines: detection limit.

Europe PMC Funders Author Manuscripts